Colloid & Polymer Science Colloid Polym Sci 272:1027–1042 (1994)

Original Contributions

Memory effects in isothermal crystallization. I. Theory

Andrzej Ziabicki and G.C. Alfonso [1])

Polish Academy of Sciences, Institute of Fundamental Technological Research, Warsaw, Poland
[1]) University of Genoa, Institute of Industrial Chemistry, Genoa, Italy

Abstract: A theoretical analysis of transient isothermal crystallization, including relaxational and athermal effects is given. The analysis is based on Kolmogoroff–Avrami–Evans transformation equation and nucleation theory of Turnbull and Fisher. The memory of previous structures manifests itself in the distribution of atomic (molecular) clusters which determines the initial number of crystal nuclei and the initial rate of thermal nucleation.

Key words: Crystallization – memory effects – nucleation – cluster distribution – relaxation times

Introduction

Memory effects are often observed in crystallization of slowly crystallizing materials, like polymers and glasses. Crystallization rate depends on original structure of the sample and its thermal history. Often, prolonged melting prior to crystallization reduces effects of the original structure.

The aim of the present analysis is explanation of memory phenomena observed in experiment, but so far discussed in intuitive, rather than systematic terms. We will show that thermal history can affect crystallization kinetics in two ways. One is melting of ordered structures remaining from previous crystallization, the other is "equilibration" of cluster distribution function. Both mechanisms contribute to the number of primary nuclei and thermal nucleation rate.

Our attention is concentrated on pure crystallizing systems, or systems containing non-crystallizing solvent. In such systems effective nuclei, whether spontaneously formed in the course of crystallization, or left from previous structures, have the same composition as the crystallizing species, and can be described with a single cluster distribution function. Our considerations do not apply to memory effects caused by "foreign" nuclei behaving in a way different from "native" ones, produced from the crystallizing material itself.

The basis for our analysis will be provided by one-dimensional theory of nucleation developed by Frenkel and Turnbull and combined with the Kolmogoroff–Avrami–Evans treatment of the kinetics of transformation. One-dimensional nucleation model is often applied to polymers though it provides a simplified picture of a more complex process. In principle, we could contemplate using a multidimensional theory of nucleation [6] for oriented polymers, and incorporate effects of *orientational relaxation* of kinetic elements. We are not doing this at the present moment. First, it would make the model much less transparent, second, we do not have at our disposal appropriate experimental data.

Part II of this research will report experimental studies of memory effects in polypropylene.

The transformation equation

For the description of transient isothermal kinetics of crystallization, we will use the statistical model proposed independently by Kolmogoroff [1], Avrami [2] and others [3, 4], commonly referred to as "Avrami model". The degree of

Table 1. Shape factors and volumes of phantom crystals

Dimensions of growth, n	Growth direction	Crystal shape	Shape factor C_n	Crystal volume v
3	R	sphere	$4\pi/3$	$4\pi R^3/3$
3	a	cube	1	a^3
2	R	cylindrical disk with thinckess d	πd	$\pi d R^2$
2	a	tetragonal plate with thickness h	h	ha^2
1	L	circular cylinder with radius r	πr^2	$\pi r^2 L$
1	h	tetragonal column with side b	b^2	$b^2 h$

transformation (crystallinity), $x(t)$, is determined by the volume of *phantom crystals*, nucleated and grown during the period $(0, t)$

$$x(t) = 1 - \exp[-E(t)] , \tag{1}$$

where

$$E(t) = -\ln[1 - x(t)] = N_0 \cdot v(0,t) + \int_0^t \dot{N}_{th}(s) \cdot v(s,t) ds . \tag{2}$$

N_0 is number of predetermined nuclei present in unit volume at the instant $t = 0$, $\dot{N}_{th}$ is thermal nucleation rate, and $v(s,t)$ is volume of a phantom crystal nucleated at the instant s and grown up to the instant t. If the growth is isotropic and proceeds independently in n dimensions, $v(s,t)$ can be expressed through the linear growth rate $\dot{R}(t)$

$$v(s,t) = C_n \cdot \left[\int_s^t \dot{R}(z) dz\right]^n . \tag{3}$$

The factor C_n for some shapes is given in Table 1.

Combination of Eqs. (1)–(3) yields logarithmic measure of the degree of transformation

$$E(t) = -\ln[(1 - x(t)] = C_n \left\{ N_0 \left[\int_0^t \dot{R}(z) dz\right]^n + \int_0^t \dot{N}_{th}(s) \cdot \left[\int_s^t \dot{R}(z) dz\right]^n ds \right\} . \tag{4}$$

A logarithmic measure of transformation (crystallization) rate results in the form

$$\dot{E}(t) = -d\ln[1 - x(t)]/dt = nC_n \left\{ N_0 \left[\int_0^t \dot{R}(z) dz\right]^{n-1} \dot{R}(t) - \int_0^t \dot{N}_{th}(s) \cdot \left[\int_s^t \dot{R}(z) dz\right]^{n-1} \dot{R}(s) ds \right\} . \tag{5}$$

When nucleation rate and linear growth rate are constants, Eq. (4) reduces to

$$E(t) = C_n \dot{R}^n [N_0 t^n + \dot{N}_{th} t^{n+1}/(n+1)] . \tag{4a}$$

Equations (4, 4a) combine two mechanisms: growth of a constant number of pre-determined nuclei, and sporadic formation and growth of new nuclei. The most often used form of the Avrami equation is written separately for isolated mechanisms

$$E(t) = K_m t^m , \tag{4b}$$

with a constant, integer exponent, $m = 1, 2$, or 3 for growth of predetermined nuclei, and $m = 2, 3, 4$ for sporadic nucleation followed by growth.

Crystallization characteristics derived from cluster distribution

The rates of nucleation and growth, as well as concentration of stable nuclei, are related to the distribution of molecular (atomic) aggregates, or clusters. For the sake of simplicity, we will consider a one-dimensional model [5, 6] in which

clusters are characterized by a single, continuous variable (reduced cluster volume) $g = v/v_0$; $g \in (1, \infty)$. The model can be used for isotropic (spherical, cubical) clusters, as well as anisotropic clusters whose shape is preserved in the process of growth (a disc or cylinder with a constant l/d ratio, tetragonal parallelepiped with constant h/a) or, growth takes place in reduced number of dimensions. Basic equations of the one-dimensional theory are discussed in Appendix A.

Cluster size distribution density, $\varrho(g,t)$, is determined by the Fokker–Planck equation

$$\frac{\partial \varrho}{\partial t} - \frac{\partial}{\partial g}\left[\mathscr{D}_{gr}\left(\frac{\partial \varrho}{\partial g} + \frac{\varrho}{kT}\frac{\partial \Delta\tilde{F}}{\partial g}\right)\right] = 0\,, \tag{6}$$

where $\Delta\tilde{F}$ denotes thermodynamic driving force for cluster formation, and $\mathscr{D}_{gr}$ is coefficient of "growth diffusion". Critical cluster size, g^*, determined by the condition

$$g = g^*: \quad \Delta\tilde{F}(g) = \text{maximum} \tag{7}$$

defines status of a nucleus. Supercritical clusters ($g > g^*$, *nuclei*) are kinetically stable: their growth, accompanied by reduction of the free energy, is preferred to dissociation. Subcritical clusters ($g < g^*$, *embryos*) are unstable and tend to reduce their size. The number of stable nuclei is calculated from the distribution function, $\varrho(g,t)$, as

$$N(t) = \int_{g^*}^{\infty} \varrho(g,t)\,dg\,. \tag{8}$$

Nucleation rate, i.e., rate of production of nuclei in the system, results from differentiation of Eq. (8):

$$\dot{N} \equiv \frac{d}{dt}\int_{g^*}^{\infty} \varrho(g,t)\,dg = \int_{g^*}^{\infty} \frac{\partial \varrho}{\partial t}\,dg - \frac{dg^*}{dt}\varrho(g^*)\,. \tag{9}$$

The first term, combined with Eq. (6) expressed as a continuity equation with flux $j(g)$

$$\frac{\partial \varrho}{\partial t} + \frac{\partial j}{\partial g} = 0 \tag{9a}$$

yields *thermal nucleation rate*:

$$\dot{N}_{th} = \int_{g^*}^{\infty} \frac{\partial \varrho}{\partial t}\,dg = \left[j(g^*) - j(\infty)\right] = -\mathscr{D}_{gr}(g^*)\left.\frac{\partial \varrho}{\partial g}\right|_{g=g^*}\,. \tag{10}$$

Note that the boundary conditions imply: $\varrho(\infty) = 0$, and $j(\infty) = 0$.

The second term, describing *athermal nucleation* [6-8], is related to the rate of change of external conditions. In non-isothermal conditions it is proportional to the rate of cooling, $\dot{T}$

$$\dot{N}_{ath} = -\frac{\partial g^*}{\partial T}\dot{T}\cdot\varrho(g^*)\,. \tag{11}$$

$\dot{N}_{ath}$ disappears in isothermal conditions, but contributes predetermined athermal nuclei when the sample is rapidly quenched. Equations (8)–(11) describe primary nucleation characteristics N_0 and $\dot{N}_{th}$ appearing in the transformation equations (4, 4a). Popular concepts of nucleation-controlled growth imply that also crystal growth rate, $\dot{R}$, is based on aggregation of molecules (atoms) into *secondary, surface nuclei.* If so, solutions for cluster distribution function (with appropriate parameters) may be used both for $\dot{N}_{th}$ and $\dot{R}$.

Equilibrium and steady-state cluster distribution

Equation (6) admits two types of solutions which are independent of time. Critical temperature for aggregation (melting, or crystallization temperature, T_m) is defined by the condition

$$T = T_m: \quad \lim_{g\to\infty} \frac{\partial \Delta\tilde{F}(g;T)}{\partial g} = 0\,. \tag{12}$$

When $T > T_m$, the flux disappears and a *Boltzmann-type, equilibrium distribution* is obtained

$$T > T_m: \left(\frac{\partial \varrho}{\partial t} = 0\right) \Leftarrow \left(j = 0\right) \Leftrightarrow \left(\varrho_{eq} = C\cdot e^{-\Delta\tilde{F}(g)/kT}\right)\,. \tag{13}$$

A natural source of the constant C is provided by normalization of mass

$$\int_1^{\infty} \varrho(g)\cdot g\,dg = \text{const}\,. \tag{14}$$

but other conditions can also be considered. When $T > T_m$, $\Delta\tilde{F}$ is positive, and asymptotically approaches $+\infty$ at $g \to \infty$. Consequently, ϱ_{eq} is always limited.

Equilibrium distribution appears in a super heated melt. For $T > T_m$, $g^* \to \infty$ and no cluster, however large, is stable:

$$N(T > T_m) = \dot{N}_{th}(T > T_m) = 0 \,. \tag{15}$$

Nevertheless, equilibrium distribution of clusters produced by prolonged heating and rapidly quenched contributes athermal nuclei active in lower temperatures. This is one of the mechanisms in which thermal history can affect crystallization.

The other time-independent solution appears when $T < T_m$. $\Delta\tilde{F}$ passes through a maximum and approaches $-\infty$ at $g \to \infty$. ϱ_{eq} calculated from Eq. (13) would be divergent and another, *steady-state distribution* must be found:

$$T < T_m: \quad \left(\frac{\partial \varrho}{\partial t} = 0\right) \Leftarrow \left(j = \text{const.} > 0\right)$$

$$\Leftrightarrow \left(\varrho_{st} = e^{-\Delta\tilde{F}/kT}\left[C_1 \int (e^{-\Delta\tilde{F}/kT}/\mathscr{D}_{gr})dg + C_2\right]\right). \tag{16}$$

Boundary conditions usually applied to the steady-state (constant flux) process, are those corresponding to an "absorbing wall"

$$\varrho_{st}(g = 1) = \varrho_1$$
$$\varrho_{st}(g = G \gg g^*) = 0 \,, \tag{17}$$

yielding

$$\varrho_{st}(g) = \frac{\varrho_1 e^{-\Delta\tilde{F}/kT} \int_g^G \left(e^{-\Delta\tilde{F}/kT}/\mathscr{D}_{gr}\right) dg'}{\int_1^G \left(e^{-\Delta\tilde{F}/kT}/\mathscr{D}_{gr}\right) dg'} \tag{18}$$

The corresponding steady-state nucleation rate yields, by combination of Eqs. (10) and (18):

$$\dot{N}_{th,st} = \frac{\varrho_1}{\int_1^G \left[e^{-\Delta\tilde{F}/kT}/\mathscr{D}_{gr}\right] dg} \,. \tag{19}$$

Transient, isothermal cluster distribution

Transient solution of Eq. (6) can be obtained by separation of variables

$$\varrho(g,t) = \sum_{i=1}^{\infty} f_i(g) e^{-\lambda_i t} \,. \tag{20}$$

If higher eigenvalues λ_i are large enough and the response time is not too short, time-dependent distribution (20) may be approximated by the first term with the smallest non-zero eigenvalue λ_1 (i.e., the longest relaxation time τ)

$$\lambda_0 = 0; \quad \lambda_1 = 1/\tau; \quad \lambda_2 = \lambda_3 = \ldots \lambda_4 = \infty \,. \tag{21}$$

The truncated series (20) with the initial condition

$$\varrho(g,0) = \varrho_0(g) \tag{22}$$

yields:

$$\varrho(g,t) \cong \varrho_{st}(g) + (\varrho_0 - \varrho_{st}) e^{-t/\tau} \tag{23}$$

$$\frac{\partial \varrho}{\partial t} \cong (\varrho_{st} - \varrho)/\tau \,. \tag{24}$$

The approximation (23), proposed in our early work [9] will be used throughout this paper.

Effects of thermal history on the distribution of clusters

Consider a sample with cluster distribution $\varrho_0(g)$ subject to a series of isothermal heating steps above melting temperature ($T_i > T_m$), followed by rapid quenching to crystallization temperature, T_{cr}. The time spent at a temperature T_i is Δt_i. The resulting distribution $\hat{\varrho}(g)$ depends on the initial structure (characterized by the original distribution ϱ_{00}), and temperature history $\{T_i, \Delta t_i\}$

$$\hat{\varrho}(g) = \hat{\varrho}[\varrho_{00}(g), T_1, \Delta t_1, T_2, \Delta t_2, \ldots T_k, \Delta t_k] \,. \tag{25}$$

To derive $\hat{\varrho}(g)$ as a functional of thermal history, we will consider the system of transient isothermal equations for individual steps of the history. Each step is characterized by temperature, T_i, relaxation time, τ_i, and equilibrium distribution, $\varrho_{eq}[g; T_i]$. We will introduce a new variable, $\xi_i = \Delta t_i/\tau_i$, i.e., reduced time spent by the material in the i-th step:

$$t = 0; \qquad \varrho_0 = \varrho_{00}$$
$$t = \xi_1; \qquad \varrho_1 = \varrho_{eq,1} + (\varrho_0 - \varrho_{eq,1}) e^{-\xi_1}$$
$$t = \xi_1 + \xi_2; \quad \varrho_2 = \varrho_{eq,2} + (\varrho_1 - \varrho_{eq,2}) e^{-\xi_2}$$
$$t = \xi_1 + \xi_2 + \ldots + \xi_{k-1};$$
$$t = \xi_1 + \xi_2 + \ldots + \xi_k;$$
$$\varrho_{k-1} = \varrho_{eq,k-1} + (\varrho_{k-2} - \varrho_{eq,k-1}) e^{-\xi_{k-1}}$$
$$\hat{\varrho} = \varrho_k = \varrho_{eq,k} + (\varrho_{k-1} - \varrho_{eq,k}) e^{-\xi_k} \,. \tag{26}$$

Multiplying k-th equation by 1, $(k-1)$-st by $e^{-\xi_k}$, $(k-2)$-nd by $e^{-(\xi_k+\xi_{k-1})}$, etc., we obtain the distribution at the end of k steps as a linear superposition of the distributions ϱ_{00}, and $\varrho_{eq,i}$

$$\varrho_k = \hat{\varrho}(g) = \varrho_{00}\exp\left(-\sum_{i=1}^{k}\xi_i\right) + \sum_{i=1}^{k}\varrho_{eq,i}\left[1-e^{-\xi_i}\right] \times \exp\left(-\sum_{p=i+1}^{k}\xi_p\right). \quad (27)$$

Fundamental characteristics of nucleation – the number of nuclei and nucleation rate – are linear functionals of the distribution function and depend on thermal history in the same way as does $\hat{\varrho}(g)$. The number of clusters which in the crystallization temperature T_{cr} behave like nuclei is:

$$N_0 = N(\hat{\varrho}; T_{cr}) = \int_{g^*(T_{cr})}^{\infty}\hat{\varrho}(g)dg = N_{00}\exp\left(-\sum_{i=1}^{k}\xi_i\right) + \sum_{i=1}^{k}N_{eq,1}\left[1-e^{-\xi_i}\right] \times \exp\left(-\sum_{p=i+1}^{k}\xi_p\right). \quad (28)$$

In a similar way, one can write thermal nucleation rate generated by the distribution $\hat{\varrho}$

$$\dot{N}_{th,0} = \dot{N}_{th}(\hat{\varrho}; T_{cr}) = -\mathscr{D}_{gr}(g^*)\left.\frac{\partial\hat{\varrho}}{\partial g}\right|_{g=g^*(T_{cr})} = \dot{N}_{th,00}\exp\left(-\sum_{i=1}^{k}\xi_i\right) + \sum_{i=1}^{k}\dot{N}_{eq,i} \times\left[1-e^{-\xi_i}\right]\exp\left(-\sum_{p=i+1}^{k}\xi_p\right). \quad (29)$$

$\dot{N}_{th,00} = \dot{N}_{th}(\varrho_{00}; T_{cr})$ denotes thermal nucleation rate at $T = T_{cr}$ controlled by the distribution function $\varrho_{00}\cdot\dot{N}_{eq,i}$ are nucleation rates at T_{cr}, generated by equilibrium distributions $\varrho_{eq,i}$.

N_0 from Eq. (28) and $\dot{N}_{th,0}$ from Eq. (29) include all information related to thermal history and represent memory effects in the subsequent crystallization.

When heating temperatures are high and/or critical cluster sizes g^* are large, equilibrium concentrations of clusters in the vicinity of g^* are very small, and in Eqs. (27–29) all terms related to $\varrho_{eq,1}$ can be neglected. Effects of heating include only gradual reduction of the initial distribution, ϱ_{00}, and Eqs. (27–29) reduce to the *relaxational term*

$$\varrho_k = \hat{\varrho} \cong \varrho_{00}\exp\left(-\sum_{i=1}^{k}\xi_i\right) \quad (27a)$$

$$N_k = N_0 \cong N_{00}\exp\left(-\sum_{i=1}^{k}\xi_i\right) \quad (28a)$$

$$\dot{N}_{th,0} = \dot{N}_{th}(\hat{\varrho}) \cong \dot{N}_{th}(\varrho_{00})\exp\left(-\sum_{i=1}^{k}\xi_i\right). \quad (29a)$$

The importance of *athermal effects*, i.e., distinction between situations described by Eqs. (27–29) vs. Eqs. (27a–29a), depends of material characteristics and crystallization temperature. When surface energy $\langle\sigma\rangle$ is high, and/or heat of melting and relative undercooling $(\Delta h\,\Delta T/T_m)$ is low, critical cluster volume $v^* = v_0\cdot g^*$ is large, and so is free energy $\Delta\tilde{F}(g^*)$. Consequently, the exponential factor $\exp[-\Delta\tilde{F}/kT]$ at, and above g^*, is close to zero, and equilibrium concentration of potential nuclei is negligible. The largest concentration of such nuclei in the state of thermodynamic equilibrium corresponds to the melting temperature, T_m. If $\varrho_{eq}(g^*; T_m)$ is negligible, effects of "equilibration" above T_m can be neglected.

We have analyzed equilibrium distributions of athermal nuclei for two materials: sodium silicate [10] and isotactic polypropylene [11]. Calculation of the critical cluster volume v^* (size, g^*) was performed for undercooling expressed as a fraction of melting temperature

$$\Delta T = (T_m - T_{cr}) = 0.1\times T_m$$

The constant c defined in Appendix A, Eq. (A8), was assumed $c = 6$, and $\langle\sigma\rangle$ was calculated as a geometric mean

$$\langle\sigma\rangle = (\sigma_1\,\sigma_2\,\sigma_3)^{1/3}$$

Molecular characteristics are given in Table 2.

It is evident that tenfold higher heat of fusion makes crystallization of inorganic silicate much easier than crystallization of polypropylene. Critical cluster size is smaller by three orders of magnitude. The equilibrium free energy, $\Delta\tilde{F}$, at $g = g^*$, and $T = T_m$, amounts to 897 kT_m for polypropylene and only 3.76 kT_m for sodium silicate. Figure 1 presents g^* and equilibrium free energy, $\Delta F(g^*; T_m)$ as a function of undercooling, and

Table 2. Crystallization characteristics for model materials

Material	Δh 10^9erg/cm^3	$\langle\sigma\rangle$ erg/cm^2	T_m K	v_0 10^{-23} cm^3	$v^*(\Delta T = 0.1\,T_m)$ 10^{-22} cm^3	Ref.
Sodium silicate	13.95	23.0	1157	4.24	2.87	[10]
Polypropylene	1.40	23.0	481.2	14.97	2837.8	[11]

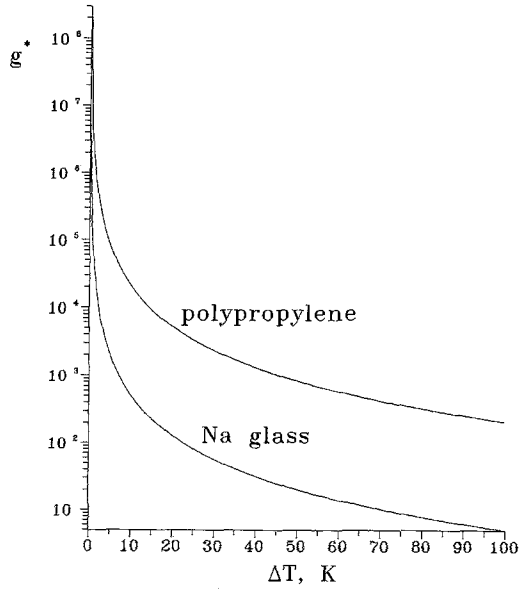

Fig. 1a. Critical cluster size, g^* as a function of undercooling, ΔT for sodium glass and isotactic polypropylene. For material characteristics see Table 2

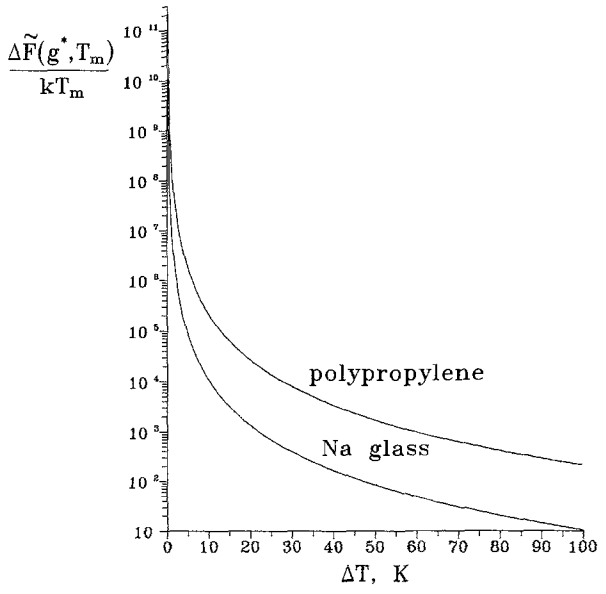

Fig. 1b. Reduced free energy $\Delta\tilde{F}(g^*, T_m)/kT_m$ as a function of undercooling, ΔT for sodium glass and isotactic polypropylene. For material characteristics see Table 2

Fig. 2 shows the equilibrium cluster density

$$\exp[-\Delta\tilde{F}(g^*; T_m)/kT]$$

and the integral

$$\int_{g^*}^{\infty} \exp[-\Delta\tilde{F}(g, T_m)/kT]\,dg$$

as functions of superheating, $T - T_m$.

Using formulas derived in Appendix A, we have

$$\Delta\tilde{F}[g^*(T_{cr}); T_m] = c\langle\sigma\rangle(v_0 g^*)^{2/3} = \frac{4(c\langle\sigma\rangle)^3}{9[\Delta h(1 - T_{cr}/T_m)]^2}\,.$$

For polypropylene, a thermodynamic barrier of the order of a thousand of kT units practically eliminates large clusters from equilibrium systems

$$(T \geq T_m; g \geq g^*) \Rightarrow (\varrho_{eq}(g) \approx 0; \dot{N}_{eq} \approx 0)\,.$$

Consequently, the mechanism consisting in "equilibration" of cluster distribution is suppressed, and memory effects are confined to relaxation mechanism. For sodium silicate, on the other hand, thermodynamic barriers are moderate, and athermal effects are comparable to relaxational ones.

Variation of the number of potential nuclei in the process of heating

Equation (28) determines the number of potential nuclei after k steps of heating. The change

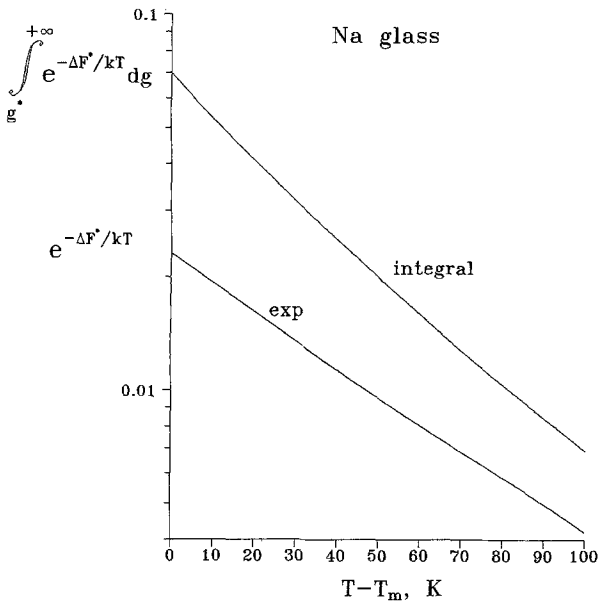

Fig. 2a. Equilibrium cluster density at $g = g^*$ as a function of superheating, $T - T_m$ for sodium glass. Critical cluster size, g^*, calculated for undercooling $\Delta T = 0.1\ T_m$. For material characteristics see Table 2

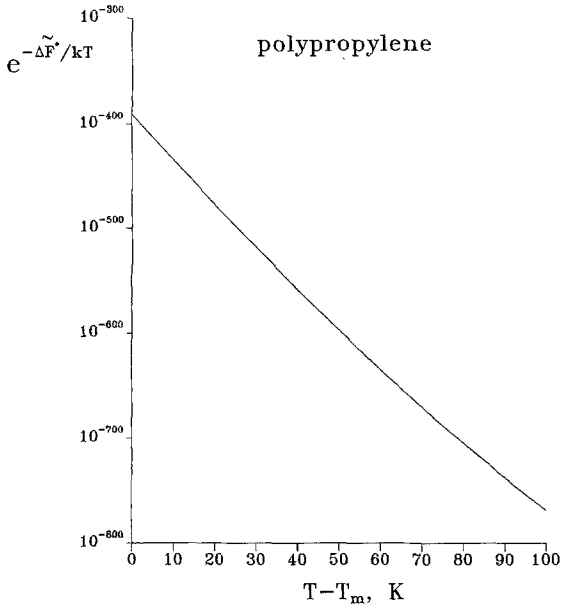

Fig. 2b. Exponential term determining cluster density in isotactic polypropylene as a function of superheating $T - T_m$. Critical cluster size, g^* calculated for $\Delta T = 0.1 T_m$. For material characteristics see Table 2

produced in k steps of heating amounts to

$$N_0 - N_{00} = N_{00}\left[\exp\left(-\sum_{i=1}^{k}\xi_i\right) - 1\right] + \sum_{i=1}^{k}\dot{N}_{eq,1}\left[1 - e^{-\xi_i}\right] \times \exp\left(-\sum_{p=i+1}^{k}\xi_p\right). \quad (30)$$

The first, *negative* term, indicates relaxational change of the original value, $\dot{N}_{00}$. Each step reduces the preceding number by a factor $e^{-\xi_i}$ dependent on temperature (T_i) and duration of heating (Δt_i). The following sum of *positive* terms accounts for athermal nuclei produced in the course of heating. Heating tends to bring cluster distribution to thermodynamic equilibrium (Eq. (13)) and contributes some amount of large clusters which behave like nuclei when the system is cooled down below T_m.

The increment of the number of potential nuclei in the i-th step of heating,

$$\Delta N_i = N_i - N_{i-1} = (N_{eq,1} - N_{i-1})[1 - e^{-\xi_i}], \quad (31)$$

can be positive or negative. ΔN is positive when equilibrium concentration corresponding to temperature T_i is higher than concentration attained in the previous step, and vice versa.

Figure 3 presents a history of temperature, and Fig. 4 gives corresponding changes of the number of potential nuclei, N_i. The history of temperature includes two steps of heating in the following arrangement:

$$T_m < T_2 < T_1, \quad (32)$$

which implies the following order of the equilibrium concentrations

$$N_{eq,1} < N_{eq,2}. \quad (33)$$

When the initial number of nuclei is high and the reduced time of heating, ξ_1, small (Fig. 4, curve a), the number of nuclei at the start of the second step of heating is higher than the equilibrium value, $N_{eq,2}$. Consequently, the number of potential nuclei will be reduced in both steps:

$$N_{00} > N_1 > N_2. \quad (34a)$$

When N_{00} is high, but heating time ξ_1 is long enough to make cluster size distribution approach equilibrium at $T = T_1$ (Fig. 4, curve b), subsequent

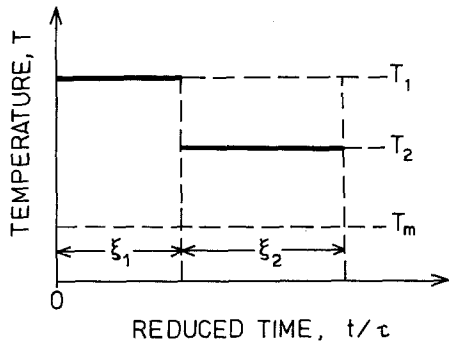

Fig. 3. Schematic changes of temperature, T, in the process of heating.

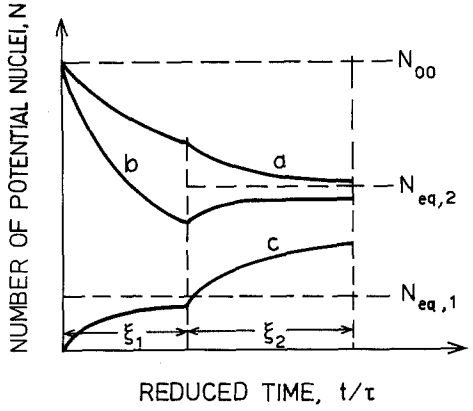

Fig. 4. Schematic changes of concentration of potential nuclei, N, in the process of heating. Individual cases (a–c) explained in the text

heating at a lower temperature leads to redistribution ("equilibration") of clusters at T_2, and N increases:

$$N_{00} > N_2 > N_1 \,. \tag{34b}$$

When the initial structure is completely free from large clusters, heating above produces, rather than removes such clusters. An example of such a behavior is shown in Fig. 4 curve c. The partial number of potential nuclei increases in both steps, more so in the lower temperature T_2:

$$0 = N_{00} < N_1 < N_2 \,. \tag{34c}$$

The above analysis indicates complex role of thermal treatment. On one hand, heating removes some clusters present in the sample. On the other hand, "equilibration" of cluster distribution produces clusters which may become athermal nuclei, when the system is quenched.

For materials with high $(\sigma/\Delta h)$ ratio, $N_{eq,i} \cong 0$, and thermal effects reduce to melting of the original clusters (Eqs. (27a–29a)). The number of potential nuclei in each consecutive step is smaller than in the preceding one (cf. inequalities (34a), and Fig. (4a)) approaching zero after prolonged heating.

Isothermal transformation with time-dependent nucleation and growth rates

The sample with initial cluster distribution ϱ_{00} is subject to thermal treatment which changes its structure to $\hat{\varrho}$. Then the sample is instantaneously transferred to a lower temperature, and crystallized at $T = T_{cr}$. Cluster distribution developed in this process can be approximated by Eq. (23). History-determined $\hat{\varrho}$ plays the role of an initial condition. Relaxation time τ_N and steady-state distribution ϱ_{st} refer to crystallization temperature. Cluster distribution in the crystallization conditions reads

$$\varrho(g,t) = \varrho_{st} + (\hat{\varrho} - \varrho_{st})e^{-t/\tau_N} \,, \tag{35}$$

and time-dependent nucleation rate at T_{cr}

$$\begin{aligned} \dot{N}_{th}(t;T_{cr}) &= \dot{N}_{th,st}(T_{cr}) \\ &\quad + (\dot{N}_{th,0} - \dot{N}_{th,st})e^{-t/\tau_N} \\ &\equiv \dot{N}_{th,st}[1 + \Delta_N e^{-t/\tau_N}] \,; \end{aligned} \tag{36}$$

Δ_N is defined as

$$\Delta_N \equiv (\dot{N}_{th,0} - \dot{N}_{th,st})/\dot{N}_{th,st} \,. \tag{37}$$

The initial values are controlled by thermal history, and the steady-state values are characteristics of crystallization temperature.

The number of predetermined nuclei present in the system at the beginning of crystallization is determined by an integral of the initial distribution function $\hat{\varrho}$, Eq. (28).

In the evaluation of time-dependent transformation equation (Eq. (4)), we will use thermal nucleation rate from Eq. (36) with the number of predetermined nuclei from Eq. (28). The appropriate time dependence of the growth rate, $\dot{R}(t)$, is not clear. The theory of nucleation-controlled

growth suggests a relation similar to that for primary nucleation (Eq. (36)). On the other hand, observation of growing spherulites indicates that linear growth rate is independent of time; it should be remembered, however, that *spherulite growth* is not necessarily identical with the *growth of crystals*. Anyway, it seems that growth rate is less sensitive to relaxational effects than primary nucleation. In this section we will discuss a combination of transient nucleation, Eq. (36), with constant growth rate

$$\dot{R}(t) = \dot{R} = \text{const} . \tag{38a}$$

Solutions for a more general case involving transient nucleation and transient growth rate

$$\dot{R}(t) = \dot{R}_{st} + (\dot{R}_0 - \dot{R}_{st})\mathrm{e}^{-t/\tau_R} \equiv \dot{R}_{st}\left[1 + \Delta_R \mathrm{e}^{-t/\tau_R}\right] \tag{38b}$$

will be given in Appendix B. Relaxation times for primary nucleation and growth are, in a general case, different. In the situation when $\tau_R \ll \tau_N$, i.e., when molecular motions involved in growth are much faster than those needed for creation of primary nuclei, Eq. (38b) reduces to (38a).

With $\dot{N}_{th}$ from Eq. (36) and constant $\dot{R}$, integration of Eq. (4) yields

$$E(t) = C_n\dot{R}^n\left\{N_0 t^n + \dot{N}_{th,st} \times \int_0^t \left(1 + \Delta_N \mathrm{e}^{-s/\tau_N}\right)(t-s)^n\, ds\right\} = C_n\dot{R}^n\left\{N_0 t^n + \dot{N}_{th,st} \times \left[t^{n+1}/(n+1) + \Delta_N \tau_N P_n(t)\right]\right\} . \tag{39}$$

The function $P_n(t)$ is shown in Appendix B, Table B1.

Two special cases of Eq. (39) are worth discussion. Consider relaxation time, τ_N, short compared with crystallization time, t. This happens *int. al.* in dilute polymer solutions (high mobility of crystallizing units) and/or at small undercooling (long crystallization time). For small τ_N/t,

$$P_n(t) = t^n[1 - n(\tau_N/t) + \ldots] , \tag{40a}$$

and the progress of crystallization reduces to

$$E(t) = C_n\dot{R}^n\left\{N_0 t^n + \dot{N}_{th,st} t^{n+1}\left[\frac{1}{n+1} + \Delta_N\left(\frac{\tau_N}{t} - \frac{n\tau_N^2}{t^2} + \ldots\right)\right]\right\} . \tag{41a}$$

For $\tau_N = 0$, Eq. (14a) reduces to Eq. (4a) in which constant nucleation rate corresponds to steady-state cluster distribution

$$\tau_N \to 0: \quad \dot{N}_{th}(t) \to \dot{N}_{th,st}[\varrho_{st}(g; T_{cr})] \quad E(t) \to C_n\dot{R}^n t^n\left\{N_0 + \dot{N}_{th,st} t/(n+1)\right\} . \tag{42}$$

When, on the other hand, τ_N is very long, $P_n(t)$ assumes the form

$$P_n(t) = \frac{n! t^{n+1}}{\tau_N}\left[\frac{1}{(n+1)!} - \frac{t}{(n+2)!\tau_N} + \frac{t^2}{(n+3)!\tau_N^2} - \ldots\right] , \tag{40b}$$

which yields

$$E(t) = C_n\dot{R}^n\left\{N_0 t^n + \dot{N}_{th,0}\frac{t^{n+1}}{n+1} - \dot{N}_{th,st}\Delta_N n! t^{n+1}\left[\frac{t}{(n+2)!\tau_N} - \frac{t^2}{(n+3)!\tau_N^2} + \ldots\right]\right\} \tag{41b}$$

At infinitely long relaxation time, Eq. (39) reduces to the same form as Eq. (4a), but nucleation rate is controlled by the initial distribution function, $\hat{\varrho}$, reflecting thermal history of the sample, in the molten state rather than crystallization temperature:

$$\tau_N \to \infty: \quad \dot{N}_{th}(t) \to \dot{N}_{th,0}[\hat{\varrho}(g; \{T_i, \xi_i\})] \quad E(t) \to C_n\dot{R}^n t^n\left\{N_0 + \dot{N}_{th,0} t/(n+1)\right\} . \tag{43}$$

Discussion

Relaxation vs. athermal effects in transient crystallization

The model of transient isothermal crystallization has been based on the theory of nucleation, and includes relaxational and athermal effects. The model accounts for the effects of thermal history of the material. Thermal treatment modifies cluster distribution, $\varrho(g)$, and affects two characteristics in the transformation equation: the number of predetermined nuclei, N_0, and the initial nucleation rate, $\dot{N}_{\mathrm{th},0}$.

The number of potential nuclei (i.e., large clusters which become athermal nuclei when the system is cooled down to crystallization temperature) changes in the process of heating in two ways. Large clusters, left from previous structures, gradually disappear. The degree of reduction depends on the history of heating. At the same time, redistribution ("equilibration") of cluster sizes may produce some amount of large clusters which become athermal nuclei on undercooling.

In materials with high interface tension, and low heat of fusion, equilibrium concentration of large clusters is negligibly small. For such materials (e.g., polypropylene and apparently other organic polymers) the *athermal mechanism* associated with "equilibration" of cluster distribution, does not contribute to the number of effective nuclei. The memory effects are controlled by *relaxation mechanism*, i.e., gradual melting of nuclei present in the system before heating. The athermal mechanism may be important for memory effects in materials with low $(\sigma/\Delta h)$ ratio, like sodium silicate, and for non-isothermal crystallization at deep undercooling.

Deviation from the "ideal" Avrami behavior. Induction time

In a general case, the progress of isothermal crystallization is a complex function of history-controlled initial conditions and relaxational phenomena (Eq. (39)). Real, isothermal transformation equation deviates from the "ideal" form (Eq. (4b)) most often used for fitting experimental data.

The first reason for discrepancy between the ideal and real behavior is *superposition of two nucleation mechanisms*, predetermined and sporadic. Even if transient effects can be neglected (i.e., relaxation time is short or long enough) the asymptotic transformation equation (Eq. (42) or (43)) can be written in the form

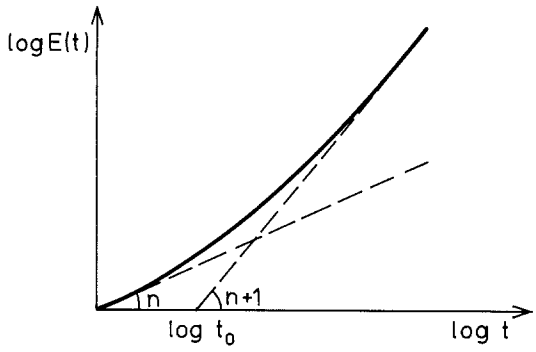

Fig. 5. Non-linear transformation as a result of superposition of predetermined and sporadic nucleation mechanisms (schematic). t_0 is induction time

$$E(t) = At^{n+1}[1 + Bt^{-1}] \,. \tag{44}$$

When presented in a traditional log E-log t plot, Eq. (45) does not produce the straight line implied by Eq. (4b), but yields

$$\log E(t) = \log A + (n+1)\log t + \log[1 + Bt^{-1}] \,. \tag{45}$$

The slope gradually changes from n for short times (predetermined nuclei) to $(n+1)$ for long times, corresponding to sporadic nucleation (Fig. 5). Fitting experimental data with a single exponent does not make much sense. The shape of the $\log E - \log t$ curve suggests introduction of an *induction time*, or *time lag*, indicating transition to the asymptotic regime. Induction times have actually been observed in some crystallization experiments [12]. Induction time, t_0, can be defined by the asymptotic relation

$$\lim_{t\to\infty}\left[\log E(t) - \frac{d\log E}{d\log t}(\log t - \log t_0)\right] = 0 \,, \tag{46}$$

and results in the form

$$\log t_0 = -\frac{\log A}{n+1} \tag{47}$$

$$A = C_n \dot{R}^n \dot{N}_{\mathrm{th,st}}/(n+1) \,, \tag{48}$$

which is controlled by steady-state nucleation rate and does not depend on the initial concentration of predetermined nuclei.

The other source of non-ideal behavior is *relaxation.* Consider isothermal crystallization controlled by sporadic, transient nucleation (Eq. (36)), and constant rate of growth in the absence of predetermined nuclei. The progress of crystallization, $E(t)$, can be written in the form

$$E(t) = \left(C_n \dot{R}^n \dot{N}_{\mathrm{th,st}}/(n+1)\right) t^{n+1} \times \left[1 + \frac{(n+1)\Delta_N \tau_N P_n(t)}{t^{n+1}}\right] = A t^{n+1}\left[1 + (n+1)\Delta_N \tau_N P_n(t)/t^{n+1}\right]. \quad (49)$$

Using asymptotic functions P_n from Eq. (40a, 40b), we arrive at the kinetic equations:

$$\log E(t) \cong \log[(1+\Delta_N)A] + (n+1)\log t - \frac{\Delta_N t}{\tau_N(1+n)(1+\Delta_N)} \cdots \quad (50a)$$

$t \to 0$:

$$d(\log E)/d(\log t) = n+1 - \frac{\Delta_N t}{\tau_N(1+n)(1+\Delta_N)} + \cdots, \quad (51a)$$

and

$$\log E(t) = \log A + (n+1)\log t + (n+1)\Delta_N \tau_N/t + \cdots \quad (50b)$$

$t \to \infty$:

$$d(\log E)/d(\log t) = n+1-(n+1) \times \Delta_N \tau_N/t + \cdots. \quad (51b)$$

The shape of the $\log E - \log t$ plot is presented in Fig. 6. Like in the superposition mechanism, the induction time calculated from Eq. (46) is identical with one described by Eq. (47)

$$t_0 = A^{-1/(n+1)} = \left((n+1)/C_n \dot{R}^n \dot{N}_{\mathrm{th,st}}\right)^{1/(n+1)}. \quad (52)$$

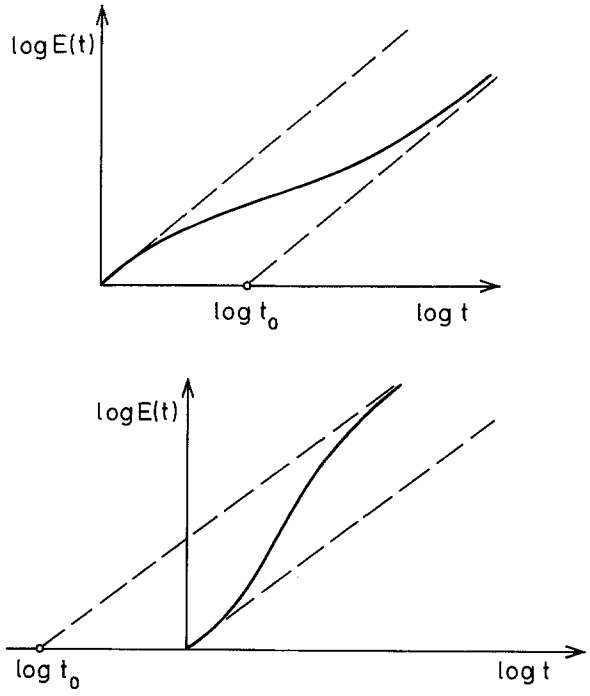

Fig. 6. Non-linear transformation as a result of transient nucleation rate. t_0 denotes induction time. a: $\Delta_N > 0$; b: $\Delta_N < 0$.

It is worth noting that the induction time does not depend on initial crystallization conditions or, in an explicit way, on relaxation time. However, nucleation and growth rates, being controlled by molecular mobility via *growth diffusion coefficient*, $\mathscr{D}_{\mathrm{gr}}$ (see Appendix A), are inversely proportional to relaxation time, τ. Therefore, the induction time is actually proportional to τ, as well as to the crystallization half-period, $t_{\frac{1}{2}}$, (cf. Eq. (54) below)

$$t_o = f(T) \cdot \tau = (\log 2)^{1/(n+1)} t_{\frac{1}{2}}. \quad (53)$$

Asymptotic crystallization and the "ideal" Avrami kinetics

Isothermal transformation equation is intrinsically transient only in the intermediate range of relaxation times. Memory of thermal history can be observed in the range of long relaxation times. Then, crystallization kinetics are determined by the *initial* number of nuclei, N_0, and *initial* nucleation rate, $\dot{N}_{\mathrm{th},0}$, both controlled by the history-sensitive cluster distribution, $\hat{\varrho}(g)$. In the range of short relaxation times, crystallization is controlled by actual (crystallization) temperature, T_{cr},

and memory effects can be neglected. We will discuss dimensionless criteria which determine the range of crystallization conditions sensitive to thermal history.

Asymptotic behavior is characterized by the ratio of relaxation time to crystallization time. The latter can be characterized by half-period of crystallization defined as

$$t = t_{\frac{1}{2}}: \quad E(t) = \log 2 \,. \tag{54}$$

When relaxation time is short compared with $t_{\frac{1}{2}}$, the progress of crystallization can be effectively described with Eq. (42), based on a constant, steady-state nucleation rate, independent of thermal history. A similar asymptotic form is obtained when relaxation time is infinitely long (Eq. (43)), with initial nucleation rate, dependent on thermal treatment.

When τ_N is comparable with $t_{\frac{1}{2}}$, the complete transformation equation (39) must be used.

To determine the range of conditions in which the "ideal" Avrami kinetics can be used, crystallization half-period must be expressed as a function of nucleation characteristics N_0, *and* $\dot{N}_{\text{th}}$. We will look for conditions converting equations (42, 43) into the "ideal", single-mechanism equation (4b) controlled by predetermined, *or* (but not *and*) sporadic nucleation. Four cases indicated in Table 3 will be analyzed.

The condition for *predetermined nucleation* as a governing mechanism, expressed through the crystallization half-period, reads

$$(n+1)N_0(t_{\frac{1}{2}})^n \gg \dot{N}_{\text{th}}(t_{\frac{1}{2}})^{n+1} \,.$$

Thermal nucleation rate is inversely proportional to relaxation time, τ_N, contained in the diffusion coefficient $\mathscr{D}_{\text{gr}}$ (cf. Eq. (A6)). Therefore, the product $(\dot{N}_{\text{th}}\tau_N)$ reflects thermodynamic factor in nucleation rate, dependent on undercooling. The condition for *predetermined nucleation* will be written in the form

$$t_{\frac{1}{2}}/\tau_N \ll \frac{N_0(n+1)}{\dot{N}_{\text{th}}\tau_N} \,, \tag{55a}$$

and that for *sporadic nucleation*

$$t_{\frac{1}{2}}/\tau_N \gg \frac{N_0(n+1)}{\dot{N}_{\text{th}}\tau_N} \,. \tag{55b}$$

Crystallization half-periods for the four asymptotic regimes are given in Table 3.

Table 3. Crystallization half-period, $t_{\frac{1}{2}}$, in asymptotic regimes

Nucleation: Predetermined	Sporadic
Relaxation time: Eq. (55a)	Eq. (55b)
$\tau_N \to 0$ $[\ln 2/C_n\dot{R}^n N_0]^{1/n}$	$[(n+1)\ln 2/C_n\dot{R}^n\dot{N}_{\text{th,st}}]^{1/(n+1)}$
$\tau_N \to \infty$ $[\ln 2/C_n\dot{R}^n N_0]^{1/n}$	$[(n+1)\ln 2/C_n\dot{R}^n\dot{N}_{\text{th,0}}]^{1/(n+1)}$

Regime 1.1. Predetermined nucleation, short relaxation time

The simultaneous conditions

$$1 \ll t_{\frac{1}{2}}/\tau_N \ll \frac{N_0(n+1)}{\dot{N}_{\text{th,st}}\tau_N} \,, \tag{56}$$

with $t_{\frac{1}{2}}$ from Table 3 yield:

$$[C_n\dot{R}^n N_0/\text{In } 2]^{1/n} \ll 1/\tau_N \ll \frac{(n+1)N_0^{(n+1)/n}}{(\dot{N}_{\text{th,st}}\tau_N)}[C_n\dot{R}^n/\text{In } 2]^{1/n} \,, \tag{57}$$

and

$$E(t) = C_n\dot{R}^n N_0 t^n \,. \tag{58}$$

The inequalities (57) call for high concentration of predetermined nuclei and large thermodynamic barrier for thermal nucleation, and lead to small value of the product $(\dot{N}_{\text{th,st}}\tau_N)$. Such conditions can be met in crystallization close to melting temperature, T_m. Effects of thermal history are included in the initial concentration of predetermined nuclei, N_0.

Regime 1.2. Sporadic nucleation, short relaxation time

The inequalities

$$1 \ll t_{\frac{1}{2}}/\tau_N \gg \frac{N_0(n+1)}{\dot{N}_{\text{th,st}}\tau_N} \tag{59}$$

yield

$$[C_n\dot{R}^n(\dot{N}_{\text{th,st}})/\text{In } 2(n+1)]^{1/n} \ll 1/\tau_N \gg \frac{(n+1)N_0^{(n+1)/n}}{(\dot{N}_{\text{th,st}}\tau_N)^{(n+1)/n}}[C_n\dot{R}^n(\dot{N}_{\text{th,st}}\tau_N)/\text{In } 2]^{1/n} \tag{60}$$

and

$$E(t) = C_n\dot{R}^n\dot{N}_{\text{th,st}}t^{n+1}/(n+1) \,. \tag{61}$$

This regime can be realized when the thermodynamic factor ($\dot{N}_{\mathrm{th,st}}\tau_N$) is rather small (low undercooling) and the number of predetermined nuclei, N_0, is very small. No effects of thermal history can be expected.

Regime 2.1. Predetermined nucleation, long relaxation time

The conditions

$$1 \gg t_{\frac{1}{2}}/\tau_N \ll \frac{N_0(n+1)}{\dot{N}_{\mathrm{th},0}\tau_N} \tag{62}$$

can be evaluated as

$$[C_n \dot{R}^n N_0/\mathrm{In}\,2]^{1/n} \gg 1/\tau_N \ll \frac{(n+1)N_0}{\dot{N}_{\mathrm{th},0}\tau_N}[C_n\dot{R}^n N_0/\mathrm{In}\,2]^{1/n}, \tag{63}$$

to yield equation $E(t)$ identical with that for regime 1.1 (Eq. (58)). To satisfy the inequalities (63), one needs large amount of predetermined nuclei, N_0. Regime 2.1. seems to provide a typical situation of crystallization at low temperatures, with strong history effects.

Regime 2.2. Sporadic nucleation, long relaxation time

The conditions

$$1 \gg t_{\frac{1}{2}}/\tau_N \gg \frac{N_0(n+1)}{\dot{N}_{\mathrm{th},0}\tau_N} \tag{64}$$

on substitution of the appropriate half-period reduce to

$$[C_n\dot{R}^n(\dot{N}_{\mathrm{th},0}\tau_N)/\ln 2(n+1)]^{1/n} \gg 1/\tau_N \gg \frac{(n+1)N_0^{(n+1)/n}}{(\dot{N}_{\mathrm{th},0}\tau_N)^{(n+1)/n}}[C_n\dot{R}^n(\dot{N}_{\mathrm{th},0}\tau_N)/\mathrm{In}\,2]^{1/n} \tag{65}$$

and, if satisfied, yield

$$E(t) = C_n\dot{R}^n\dot{N}_{\mathrm{th},0}t^{n+1}/(n+1). \tag{66}$$

It is not clear whether the conditions (65) can ever be realized. The ineqalities stipulate large ratio of the initial nucleation rate to concentration of predetermined nuclei. We will try to estimate this ratio for equilibrium distribution of clusters. Using rough, linear estimate of the integral

$$N_0 = \int_{g^*}^{\infty} \varrho_{\mathrm{eq}}(g)dg = C\int_{g^*}^{\infty}\exp[-\Delta\tilde{F}(g)/kT]dg \cong \tfrac{1}{2}C\cdot kT\exp[-\Delta\tilde{F}(g^*)/kT]/(d\Delta\tilde{F}/dg)_{g^*}, \tag{67}$$

and realizing that thermal nucleation rate for equilibrium distribution reduces to

$$\dot{N}_{\mathrm{th}}[\varrho_{\mathrm{eq}}(g)] = -\mathscr{D}_{\mathrm{gr}}(g^*)(\partial\varrho_{\mathrm{eq}}/\partial g)_{g^*} = C\mathscr{D}_{\mathrm{gr}}(g^*)\exp[-\Delta\tilde{F}(g^*)/kT]\cdot(d\Delta\tilde{F}/dg)_{g^*}/kT, \tag{68}$$

we obtain the ratio

$$\dot{N}_{\mathrm{th}}[\varrho_{\mathrm{eq}}(g)]\cdot\tau/(n+1)N_0[\varrho_{\mathrm{eq}}(g)] \cong 2\mathscr{D}_{\mathrm{gr}}(g^*)\cdot\tau(d\Delta\tilde{F}/dg)^2_{g^*}/(kT)^2 \tag{69}$$

and, substituting $\mathscr{D}_{\mathrm{gr}}$, g^*, and $\Delta\tilde{F}$ from Appendix A

$$\dot{N}_{\mathrm{th}}\tau/(n+1)N_0 \cong \frac{8}{9}D_0\left[\frac{c\langle\sigma\rangle v_0^{2/3}}{kT_m}\right]^2\left(\frac{T_m}{T}\right)\times\left(\frac{T-T_{\mathrm{cr}}}{T_m-T_{\mathrm{cr}}}\right)^2. \tag{70}$$

The ratio of initial nucleation rate to the concentration of predetermined nuclei can assume arbitrarily high values when crystallization is carried out in the vicinity of melting temperature. It seems that the existence of regime 2.2, is justified by long relaxation times combined with small undercooling ($T_{\mathrm{cr}} \approx T_m$), though the combination does not seem common.

Two, out of four asymptotic regimes seem natural. Sporadic nucleation with short relaxation times (regime 1.2) can be expected in systems with high molecular mobility (crystallization from solutions). Memory effects disappear at the beginning of the process, and thermal history does not influence the isothermal process. On the other hand, predetermined nucleation with long relaxation times is strongly sensitive to thermal history. Regime 2.1 can be expected in systems with long relaxation times, large concentration of predetermined nuclei, and crystallization temperatures not too close to the melting temperature, T_m. History effects concern the amount of predetermined nuclei, N_0, rather than initial nucleation rate, $\dot{N}_{\mathrm{th},0}$.

Appendix A

Basic equations of one-dimensional nucleation theory [5, 6]

The theory considers kinetics of a set of *reversible reactions of association and dissociation*

$$\beta_{g-1} + \beta_1 \underset{k_g^-}{\overset{k_{g-1}^+}{\rightleftharpoons}} \beta_g \,, \tag{A1}$$

$g = 2, 3, \ldots$ denotes *cluster size*, i.e., number of single kinetic elements contained in a cluster β_g. The *discrete flux* of association expressed by molar fractions of the reacting species reads

$$j_g = k_{g-1}^+ [\beta_{g-1}] \cdot [\beta_1] - k_g^- [\beta_g] \,. \tag{A2}$$

The ratio of reaction rate coefficients is assumed as one in thermodynamic equilibrium, i.e.,

$$k_{g-1}^+ / k_g^- = \exp[-\Delta\mu_{0,g}/kT] \,, \tag{A3}$$

where the difference of standard chemical potentials, expressed by molecular free energies of individual species, and the total driving force, $\delta\tilde{F}$, for aggregation at concentration $[\beta_1]$, read

$$\begin{aligned} \Delta\mu_{0,g} &= F_g - F_{g-1} - F_1 \\ \delta\tilde{F}(g) &= \Delta\mu_{0,g} - kT \ln[\beta_1] \,. \end{aligned} \tag{A4}$$

Equations (A2)–(A4) can be solved, yielding discrete cluster size distribution, $[\beta_g]$. It is convenient, however, to use continualized solutions which have been shown to be equivalent to the exact discrete solutions. Continualization of the variable g, replacement of molar fractions $[\beta_g]$ by density in the space of cluster sizes, $\varrho(g)$, and linearization of the resulting expressions yields *continuous flux* in the space g

$$\begin{aligned} j(g) &= k_g^- [e^{-\delta\tilde{F}/kT} \varrho(g-1) - \varrho(g)] \\ &\cong -k^-(g)[\partial\varrho/\partial g + (\varrho/kT)\partial\Delta\tilde{F}/\partial g] \\ &= -\mathscr{D}_{gr}[\partial\varrho/\partial g + (\varrho/kT)\partial\Delta\tilde{F}/\partial g] \,. \end{aligned} \tag{A5}$$

The integral, $\int\delta\tilde{F}(g)dg = \Delta\tilde{F}(g)$, provides the thermodynamic driving force for "diffusional growth" of clusters.

Continuity equation for cluster-size distribution, $\varrho(g,t)$, based on the flux from Eq. (A5), assumes the form of a Fokker–Planck equation discussed in this paper as Eq. (6).

The flux $j(g)$ has a diffusional structure, and the continualized dissociation rate, $k^-(g)$, is identified with *diffusion coefficient in the space of cluster sizes*, or coefficient of "growth diffusion". $\mathscr{D}_{gr}$ can be presented in the form

$$\begin{aligned} k^-(g) \equiv \mathscr{D}_{gr}(g;T) &= \text{const.}\,(T) g^{2/3} e^{-E_\eta/kT} \\ &= D_0(T/T_m) g^{2/3}/\tau \,; \end{aligned} \tag{A6}$$

E_η denotes activation energy for self-diffusion of the kinetic units subjects to aggregation, and τ is the related relaxation time. The factor $g^{2/3}$ accounts for the number of sites available for the reactions of association and dissociation on the surface of a g-size cluster. Temperature-dependent front factor is related to natural frequency of molecular motions participating in the reaction.

Continualized *free energy of transition* of g single kinetic elements into a g-size cluster is assumed in the form:

$$\begin{aligned} \Delta F(g) = F_g - g \cdot F_1 &= (-\Delta h + T\Delta s_0) v_0 g \\ &\quad + c\langle\sigma\rangle (v_0 g)^{2/3} \,. \end{aligned} \tag{A7}$$

The total *driving force*, including free energy of mixing of untransformed single elements

$$\begin{aligned} \Delta\tilde{F}(g) &= \Delta F(g) - (g-1) v_0 kT \ln\varrho_1 \\ &= -(g-1) v_0 kT \ln\varrho_1 - (\Delta h - T\Delta s_0) v_0 g \\ &\quad + c\langle\sigma\rangle (v_0 g)^{2/3} \,. \end{aligned} \tag{A8}$$

Δh denotes heat of fusion per unit volume, $\langle\sigma\rangle$-average surface energy density (interface tension), Δs_0-entropy of crystallization for an undiluted system ($\varrho_1 = 1$), T – crystallization temperature, v_0-molecular volume of a single kinetic element and c is a dimensionless constant dependent on cluster shape. For spherical clusters, $c = (36\pi)^{1/3}$, for cubes, or proportionally growing parallelepipeds, $c = 6$, etc.

Critical crystallization (melting) temperature is obtained from the condition:

$$T = T_m: \quad \lim_{g\to\infty} \frac{\partial\Delta\tilde{F}}{\partial g} = 0 \,, \tag{A9}$$

yielding

$$T_m = \frac{\Delta h}{\Delta s} = \frac{\Delta h}{\Delta s_0 - k\ln\varrho_1} \,. \tag{A10}$$

Δs is complete entropy of the transition including mixing term. With T_m from Eq. (A10), the driving

force $\Delta\tilde{F}(g)$ can be written as

$$\Delta\tilde{F}(g) = c\langle\sigma\rangle(v_0 g)^{2/3} - (g-1)v_0 kT\ln\varrho_1 - \Delta h(1-T/T_m)v_0 g\,. \tag{A11}$$

Critical cluster size, g^*, is obtained from the condition:

$$g = g^*(T):\quad \frac{\partial\Delta\tilde{F}(g;T)}{\partial g} = 0\,, \tag{A12}$$

which yields

$$v_0 g^*(T) = \left[\frac{2c\langle\sigma\rangle}{3\Delta h(1-T/T_m)}\right]^3, \tag{A13}$$

and

$$\frac{dg^*}{dT} = \frac{3g^*}{T_m - T}\,. \tag{A14}$$

Maximum driving force, $\Delta\tilde{F}_{\max}$, at a temperature, T, below melting temperature T_m, provides the thermodynamic barrier for nucleation

$$\Delta\tilde{F}_{\max} = \Delta\tilde{F}(T, g^*(T)) = \frac{4}{27}\frac{(c\langle\sigma\rangle)^3}{[\Delta h(1-T/T_m)]^2}\,. \tag{A15}$$

Appendix B

Transformation equation involving transient nucleation and/or transient growth rates

Integration of Eq. (4) with transient nucleation rate (eq. 36) and transient growth rate (Eq. 38b) yields

$$\begin{aligned} E(t) &= C_n\dot{R}_{st}^n\{N_0[t+\Delta_R\tau_R(1-e^{-t/\tau_R})]^n \\ &\quad + \dot{N}_{th,st}\int_0^t(1+\Delta_N e^{-s/\tau_N})[t-s+\Delta_R\tau_R \\ &\quad \times(e^{-s/\tau_R}-e^{-t/\tau_R})]^n ds\} \\ &= C_n\dot{R}_{st}^n\{N_0[t^n+\Delta_R\tau_R Q(t)] \\ &\quad + \dot{N}_{th,st}[t^{n+1}/(n+1)+\Delta_N\tau_N P_n(t) \\ &\quad + \Delta_R\tau_R S(t)] \end{aligned} \tag{B1}$$

Functions $P(t)$, describing transient nucleation at constant growth rate are defined as

$$P_n(t) = \{\int_0^t(1+\Delta_N e^{-s/\tau_N})(t-s)^n ds - t^{n+1}/(n+1)\}/\Delta_N\tau_N\,, \tag{B2}$$

Table B1. Transient nucleation functions $P_n(t)$

Dimensions of growth, n	Function P_n
3	$t^3 - 3t^2\tau_N + 6t\tau_N^2 - 6\tau_N^3(1-e^{-t/\tau_N})$
2	$t^2 - 2t\tau_N + 2\tau_N^2(1-e^{-t/\tau_N})$
1	$t - \tau_N(1-e^{-t/\tau_N})$

Table B2. Transient growth functions $Q_n(t)$

Dimensions of growth, n	Function Q_n
3	$(1-e^{-t/\tau_R})[3t^2 + 3t\Delta_R\tau_R(1-e^{-t/\tau_R}) + \Delta_R^2\tau_R^2(1-e^{-t/\tau_R})^2]$
2	$(1-e^{-t/\tau_R})[2t + \Delta_R\tau_R(1-e^{-t/\tau_R})]$
1	$(1-e^{-t/\tau_R})$

and read

$$P_n(t) = (-1)^n n!\tau_N^n(1-e^{-s/\tau_N}) + \sum_{k=1}^{n}(-1)^{n-k}\frac{n!}{k!}t^k\tau_N^{n-k}\,. \tag{B3}$$

Individual function P_n for $n = 1, 2, 3$ are shown in Table B1.

The functions $Q_n(t)$ describe transient growth of predetermined nuclei

$$\begin{aligned} Q_n(t) &= \{[t+\Delta_N\tau_R(1-e^{-t/\tau_R})]^n - t^n\}/\Delta_R\tau_R \\ &= \sum_{k=1}^{n}\binom{n}{k-1}(1-e^{-t/\tau_R})^{n-k+1}(\Delta_R\tau_R)^{n-k}t^{k-1}. \end{aligned} \tag{B4}$$

Individual functions Q_n are listed in Table B2.

Functions $S_n(t)$ describe sporadic (transient) nucleation combined with transient growth rate. Individual functions read:

$$\begin{aligned} S_1(t) = &-te^{-t/\tau_R} + \tau_R\left(1+\frac{\Delta_N\tau_N}{\tau_N+\tau_R}\right) \\ &-(\tau_R+\Delta_N\tau_N)e^{-t/\tau_R} + \frac{\Delta_N\tau_N^2}{\tau_N+\tau_R}e^{-t/\tau_R}e^{-t/\tau_N} \end{aligned} \tag{B5}$$

$$
\begin{aligned}
S_2(t) = & -t^2 e^{-t/\tau_R} + t\cdot\tau_R\left[2\left(1+\frac{\Delta_N\tau_N}{\tau_R+\tau_N}\right)\right. \\
& \left.+e^{-2t/\tau_R}\right] - \tau_R^2\left[\frac{3}{2}+2\frac{\Delta_N\tau_N}{\tau_R+2\tau_N}\right. \\
& \left.-\frac{\Delta_N\tau_N\Delta_R}{\tau_R+\tau_N}\right] + 2\Delta_N\tau_N e^{-t/\tau_R} \\
& \times\left[\tau_N-\tau_R-\frac{\Delta_R\tau_R^2}{\tau_R+\tau_N}\right] + \frac{3}{2}\tau_R^2 e^{-2t/\tau_R} \\
& + \Delta_N\tau_N e^{-t/\tau_R} e^{-t/\tau_N}\left[\frac{2(\tau_R^2-\tau_N^2-\tau_N\tau_R)}{\tau_R+\tau_N}\right. \\
& \left.+\Delta_R\tau_R\right] - 2\Delta_N\tau_N^3\Delta_R\tau_R \\
& \times e^{-2t/\tau_R} e^{-t/\tau_N}\frac{1}{(\tau_R+\tau_N)(\tau_R+22\tau_N)} \qquad \text{(B6)}
\end{aligned}
$$

$$
\begin{aligned}
S_3(t) = & -t^3 e^{-t/\tau_R} + 3t^2\tau_R \\
& \times\left\{1+\frac{\Delta_N\tau_N}{\tau_R+\tau_N}-\frac{\Delta_N\tau_N}{\tau_R}e^{-t/\tau_R}+\frac{\Delta_R}{2}e^{-t/\tau_R}\right\} \\
& + t\left\{\left[-\frac{9}{2}\tau_R^2+\frac{3\Delta_N\tau_N\Delta_R\tau_R^2}{\tau_R+2\tau_N}-\frac{6\Delta_N\tau_N^2\tau_R^2}{(\tau_R+\tau_N)^2}\right]\right. \\
& - 6e^{-t/\tau_R}\left[\tau_R^2-\Delta_N\tau_N^2+\frac{\Delta_N\tau_N\Delta_R\tau_R^2}{\tau_R+\tau_N}\right] \\
& \left.+ 3\Delta_N\tau_N\Delta_R\tau_R e^{-2t/\tau_R} - \Delta_R^2\tau_R^2 e^{-3t/\tau_R}\right\} \\
& + \tau_R^3\left[\frac{21}{4}+\frac{\Delta_R^2}{3}+\frac{6\Delta_N\tau_N^3}{(\tau_R+\tau_N)^3}-\frac{3\Delta_N\tau_N^2\Delta_R}{(\tau_R+2\tau_N)^3}\right. \\
& \left.+\frac{\Delta_N\tau_N\Delta_R^2}{\tau_N+3\tau_N}\right] - e^{-t/\tau_R}\left\{\frac{3\Delta_R^2\tau_R^3}{2}+6\Delta_N\tau_N^3\right. \\
& \left.- 3\Delta_N\tau_N\Delta_R\tau_R^3\left[\frac{2\tau_N}{(\tau_R+\tau_N)^2}-\frac{\Delta_R}{\tau_R+2\tau_N}\right]\right\} \\
& - 3\Delta_R e^{-2t/\tau_R}\left\{\frac{7\tau_R^3}{4}-\Delta_R\tau_R^3+\Delta_N\tau_N^2\tau_R\right. \\
& \left.-\frac{\Delta_N\tau_N\Delta_N\tau_R^3}{\tau_R+\tau_N}\right\} - \Delta_R^2\tau_R^2 e^{-3t/\tau_R}\left[\frac{11\tau_R}{6}\right. \\
& \left.+\Delta_N\tau_N\right] + 6\Delta_N\tau_N^3 e^{-t/\tau_R} e^{-t/\tau_N} \\
& \times\left[1-\frac{\tau_R^3}{(\tau_R+\tau_N)^3}\right] \\
& + 3\Delta_N\tau_N^2\Delta_R\tau_R^3 e^{-2t/\tau_R} e^{-t/\tau_N} \\
& \times\left[\frac{1}{(\tau_R+2\tau_N)^2}-\frac{2}{(\tau_R+\tau_N)^2}\right] \\
& + \Delta_N\tau_N\Delta_R^2\tau_R^3 e^{-3t/\tau_R} e^{-t/\tau_N} \\
& \times\left[\frac{1}{\tau_R}-\frac{3}{\tau_R+\tau_N}+\frac{3}{\tau_R+2\tau_N}-\frac{1}{\tau_R+3\tau_N}\right] \qquad \text{(B7)}
\end{aligned}
$$

References

1. Kolmogoroff AN (1937) Izvestiya Akademii Nauk SSSR, Ser Math 3:335
2. Avrami M, J Chem Phys 7:1103 (1939); ibid 8:212 (1940); ibid 9:177 (1941)
3. Evans UR (1945) Trans Faraday Soc 41:365
4. Johnson WA, Mehl RF (1939) Trans AIME 135:416
5. Turnbull D, Fisher JC (1949) J Chem Phys 17:71
6. Ziabicki A (1986) J Chem Phys 85:3042
7. Fisher JC, Hollomon JH, Turnbull DJ (1948) Appl Phys 19:775
8. Ziabicki AJ (1968) Chem Phys 66
9. Ziabicki A, IUPAC Symposium on Macromolecules, Prague 1965, preprint p-344
10. Coenen M (1964) Kolloid Z 194:136
11. Monasse B, Haudin JM (1986) Colloid & Polymer Sci 264:117
12. Colomer Vilanova P, Monserrat Ribes S, Martin Guzman G (1985) Polymer 26:423

Received September 6, 1993;
accepted January 28, 1994

Address for correspondence:

Professor A. Ziabicki
Polish Academy of Sciences
21 Świętokrzyska St., PL-00049 WARSZAWA, Poland
Professor Giovanni Carlo Alfonso
Universita di Genova
Istituto Chimica Industriale
Corso Europa 30
I-16132 GENOVA, Italy